Electronic and positronic states in YBa$_2$Cu$_4$O$_8$

Electronic and positronic states in YBa$_2$Cu$_4$O$_8$

B Barbiellini and T Jarlborg

DPMC, Université de Genève, CH-1211 Genève 4, Switzerland

Abstract. LMTO calculations have been done in order to obtain electronic and positronic states in YBa$_2$Cu$_4$O$_8$. The annihilation rates have been calculated including the enhancement effects. Theoretical momentum density spectra are used for prediction of Fermi surface signals.

1. Introduction

Band calculations show that positrons in YBaCuO compounds are good probes of Cu–O chain-related electronic states (see for example [1,2]). Therefore clear Fermi surface (FS) signals related to these states should be seen. Experimentally these FS structures have escaped observation for a long time in YBa$_2$Cu$_3$O$_{7-\delta}$ (1:2:3) [3]. A possible explanation of the difficulty in observing a clear FS signal in 1:2:3 is that the Cu–O chains give smaller signals in less oxygenated and Al contaminated samples than in an ideal pure sample [22]. Recent measurements have shown signals of the ridge in the 1:2:3 oxide [4–6].

The YBa$_2$Cu$_4$O$_8$ (1:2:4) superconductor may be a better candidate since the oxygen content is stable [7] and it forms twin-free crystals. Higher binding energy of the chain oxygen atom has also been deduced from recent electronic calculations [8–10]. Therefore, we have studied the 1:2:4 structure in order to determine the amplitudes of the positron annihilation signal.

In the present work we calculate the electronic structure self-consistently by use of our linear muffin-tin orbital (LMTO) method [11]. The positronic structure is calculated in the potential field which is set up by the electron density. In the calculations of the electron–positron annihilation spectra, we employ the so-called independent particle model (IPM) as well as the enhancement effects. The results are tested for sensitivity to different approximations in order to obtain a prediction for the form of angular correlation of annihilation radiation (ACAR) spectra. It turns out that the ridge structure of the Fermi surface should come out as clearly as in the 1:2:3 compound, while the pillbox FS is absent, and the barrel structure escapes detection due to the weak positron distribution around the corresponding sites.

2. Method

Self-consistent calculations of the electronic structure have been performed using the LMTO method within the local density approximation (LDA). The core-electron configurations are: Ba:(Kr) (4d^{10}) (5s^2), Y:(Kr), Cu:(Ar) and O:(H). The

wavefunctions were expanded with the spherical waves up to the angular momentum $l = 2$ inside the overlapping spheres around ions and angular momentum $l = 1$ around empty spheres. We use the crystal structure, lattice constants, internal position and notation of ions listed in [8]. One empty sphere is at the missing oxygen at the chain level, and one other is inserted in the plane containing Y. Various choices of sphere radii were tested in calculations of the electronic structure, and the values that were finally chosen are given in table 1; with this choice the results for stability, band dispersions and potential steps at the radii were satisfactory.

The positron potential is taken as the inverse of the electron Coulomb potential. Singh *et al* [13] have shown, using accurate full potential calculations, that the inclusion of correlation is important in the BiSrCaCuO compound but not in the YBaCuO. The region sampled by the positron is essentially the same as when the positron–electron correlation potential is neglected. Moreover, our experience [14] is that, with the atomic sphere approximation (used in LMTO), the inclusion of the positron–electron correlation potential may give some exaggerated charge transfer from empty to atomic spheres in the case of compounds. This is why we leave it out.

The positron is assumed to be thermalized when annihilating and its wavefunction is calculated near $k = 0$. The delocalized positron, described by its one-particle wavefunction, has negligible effect on the average electron distribution, so no electron–positron *self-consistency* is needed. We perform the positron band calculation using an LMTO basis of s and p orbitals only, while choices of spheres, their radii etc, are as in the electronic calculation.

The two photon momentum distribution (TPMD), with an enhancement factor $\gamma(r_s(r))$ (due to electron–positron Coulomb attraction) as in a local density approach, is given by [12]

$$\rho(p) = \text{constant} \times \sum_{\text{occ}} \left| \int d^3 r \exp(-ipr) \psi^+(r) \psi_{k,n}(E,r) \sqrt{\gamma(r_s(r))} \right|^2 \qquad (1)$$

and the zone-reduced momentum density can be reduced to [15]

$$R(k) = \sum_G \rho(k-G) = \text{constant} \times \int d^3 r \, \gamma(r) |\psi^+(r)|^2 n(k,r) \qquad (2)$$

where $R(k)$ and $n(k,r)$ are respectively the positron annihilation rate and the electron density arising from occupied electronic states at k. If γ is unity, one has the IPM condition, and if additionally $\psi^+ = \text{constant}$, one obtains the electron momentum density (EMD) in the reduced space as in the Lock–Crisp–West (LCW) theorem [16]. Actually $R(k)$ varies for different k and the FS structures are modulated by wavefunction and enhancement effects. The Bloch states are obtained from an LMTO calculation. Formula ((2)) leads to significant computational simplification. However, to compare theory with extended zone experimental data, formula ((1)) must be used. Singh and Jarlborg [17] first used the LMTO method to calculate TPMD. The results were satisfactory for the first Brillouin zone even when no corrections to the overlapping sphere geometry were made. These authors derived an efficient method to correct the overlapping spheres which produces good results for umklapp processes too. This correction for the overlapping spheres can be used to calculate the positron density distribution using the corrected Fourier components. Finally the

total annihilation rate (i.e. the inverse of the positron lifetime τ) is obtained by summing over all momenta and is computed using the formula [14]

$$\frac{1}{\tau} = \text{constant} \times \int d^3r \; \gamma(r)|\psi^+(r)|^2 n(r). \tag{3}$$

This expression is very sensitive to the description of the enhancement factor [2, 14]. Normally the correlation potential affects the lifetime as well, since the positron real-space distribution is changed. Rojas *et al* [18] found that at most a difference of 10 ps occurred in low-density semiconductors, when positron–electron correlation was included. However, in the present case, the density is higher and, as discussed above, full potential calculations [13] show that the positron distribution should not change significantly when positron–electron correlation is included.

3. Results

3.1. Electronic structure

Figure 1 shows the bandstructure calculated at 50 k-points in an orthorhombic zone (the labels are made to be compatible with those of the simple orthorhombic structure for YBa₂Cu₃O₇ [9]). Compared to the 1:2:3 compound, the FS is now changed so that no pillbox appears. At the S-point no bands approach closer than about 40 mRyd to the Fermi level, so in contrast to the 1:2:3 compound, small shifts of E_F cannot make the pillbox appear or disappear. However, the barrel bands, mostly coming from the Cu–O plane, are present as in 1:2:3. Now two ridge bands exist, instead of only one as in 1:2:3. This is understood from the fact that twice as many Cu–O chains exist in the 1:2:4 structure compared to 1:2:3, and that the ridge FS is associated with these chains. The EMD projected along c is shown in figure 2 and the breaks correspond to the four sheets of the FS.
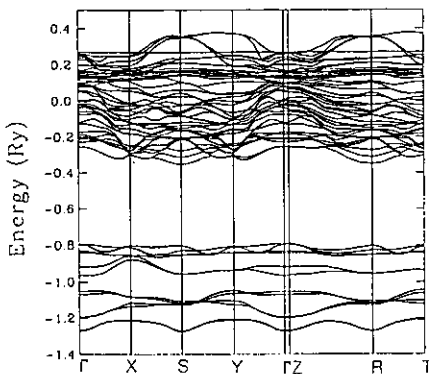

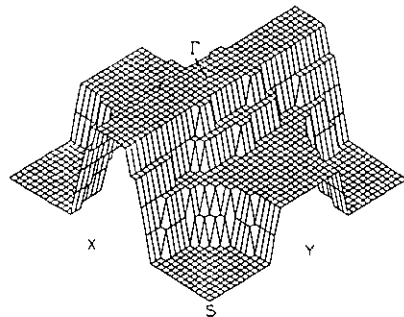**Figure 1.** Energy bands of YBa₂Cu₄O₈ (Fermi level is indicated).

Figure 2. Electron momentum density projected along c. The labels are made to be compatible with those of the simple orthorhombic Brillouin zone.

Good agreement for energy bands is found among all the full potential calculations [8–10]. However, the oxygen core-level shifts studied in [10] differ from those of [9]. These discrepancies could come from computational differences such as the choice of different oxygen sphere radii [10]. The atomic sphere approximation used in LMTO can also modify the bandstructure. However, the FS is similar in all the calculations, and our FS is sufficiently precise to allow reliable momentum density studies.

Table 1 displays the site decomposition of the density of states (DOS) at the Fermi level $N(E_F)$. These results are similar to those for the 1:2:3 compound [19], although the total DOS is smaller. This indicates that the replacement of the pillbox by a second ridge provides fewer states near E_F. Another difference is that the oxygens in the chains have smaller partial DOS than is the case in the 1:2:3 compound. The reason for this has to be sought in the difference in geometry around the chains. In 1:2:3, the Cu(1) is symmetrically surrounded by the bridging oxygens, while here Cu(1) has another Cu(1) on one side, opposite to the bridging oxygen. The local Cu DOS is somewhat larger in 1:2:4 than in 1:2:3.

Table 1. Wigner–Seitz radii, partial DOS at E_F and relative positron density (normalized as one positron per unit cell) within the different sites. The structural data are taken from [8], and the site notations are such that Cu(2), O(2) and O(3) form the planes, while Cu(1), O(1) and O(4) form the chains (O(4) is the apical oxygen between planes and chains). The empty sphere E(1) is on a missing oxygen site, and E(2) is in the Y-plane.

Site	R_{WS} (au)	$N(E_F)$ (Ryd cell)$^{-1}$	Positron density (10^3au^{-3})
Y	3.4973	0.4	0.0
2Ba	3.6971	2.5	0.2
2Cu(1)	2.4981	18	1.8
2Cu(2)	2.4981	15	0.0
2O(2)	2.2981	3.7	0.0
2O(3)	2.2981	4.4	0.0
2O(1)	2.1983	9.6	1.5
2O(4)	2.2981	4.9	0.2
2E(1)	2.1983	0.3	6.0
E(2)	1.7408	0.1	0.0

3.2. Positronic structure

Table 1 also shows the relative positron density as it is obtained from the lowest band near the Γ point. The large electron positron overlap for the chain region suggests that FS breaks that are contained in ACAR spectra should come from the chains, and consequently from the ridge bands. In contrast, detection of barrel bands should be difficult, since the positrons avoid the plane region. In figure 3, we show the positron densities in two sections of the unit cell, as obtained from a plane wave projection of the Wigner–Seitz sphere densities with overlap corrections as described in [17]. The strong build-up of positron density in the chain region is evident. It is also found that the positron density is high in open spaces of the structure at the positions of empty spheres, where the electron potential is repulsive. But it also shows rather flat densities in open regions that have not been included within empty spheres, as is the case for the central point in figure 3(*b*). For the electronic structure calculation it is not very crucial to have empty spheres everywhere near open spaces, since the
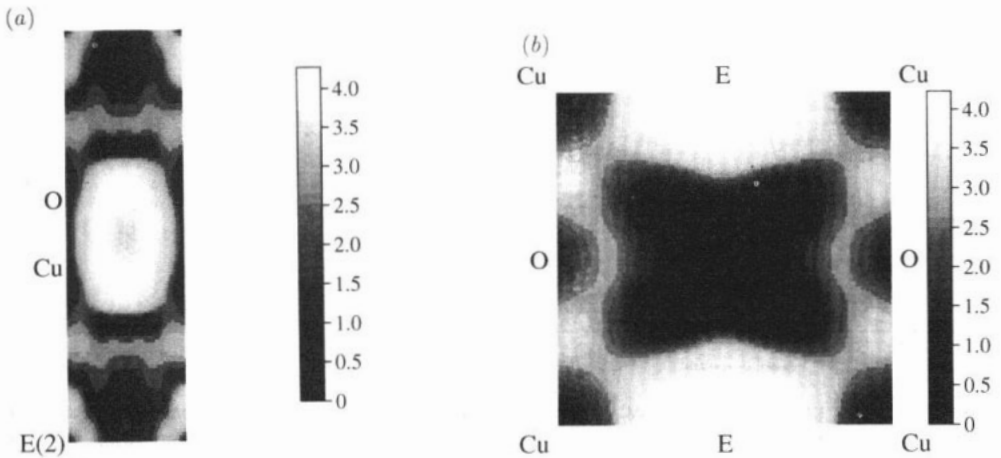
Figure 3. Grey scale positron density distribution (arbitrary units) in (*a*) an *x–z* vertical plane containing the E(2), Cu(1), O(1) sites and in (*b*) a Cu–O chain layer (E indicates an empty site).

electronic functions are peaked on atomic sites. But in retrospect it seems that the inclusion of more empty spheres would have been advantageous for the description of the positron density, although for the annihilation it is of less importance since the electron–positron *overlap* is probed. In view of the difficulty of handling more spheres in repeated electronic and positronic band calculations, we have analysed ACAR spectra by using the present band results and estimated the sensitivity due to modifications of the positron density.

The calculated positron lifetimes (in ps) are 156 for 1:2:3 (if $\delta = 0$) and 183 for 1:2:4. The experimental lifetimes for 1:2:3 and 1:2:4 are respectively 170 ± 5 and 198 ± 5 [20]. The different τ in the two compounds can be understood by the fact that more open space exists in the 1:2:4 (chain layers). In 1:2:3, when δ increases, the lifetime increases, reaching a calculated value of 200 ps and an experimental one of 215 ± 5 ps for $\delta = 1$ [20]. This is explained by the tendency for positrons to localize in the oxygen-deficient zones [21].

3.3. Calculations of annihilation spectra

The *c*-axis projections of the ACAR spectra calculated with and without enhancement, are shown in figure 4. The inclusion of the enhancement effect makes the calculated ACAR more peaked near $p = 0$. This is a result of the more extended annihilation in real space (via $\gamma(r)$).

The predicted *c*-projected momentum density in the reduced *k*-space (LCW folding) is shown in figure 5 and appears comparable to the corresponding picture for the 1:2:3 compound, except that the small downward bending in the corners due to the pillbox is absent. The amplitude of the modulation amounts to 10% of the constant background. In the 1:2:4 the Cu–O ridge signal is larger by a factor of almost two with respect to 1:2:3 and should allow for experimental detection. The relatively stronger FS signal is to a large extent due to the fact that 1:2:4 has two ridge FS instead of one. The signal of the barrel FS is weak, and it is probably not detectable. Finally the folded momentum $R(k)$ does not depend crucially on the exact shape
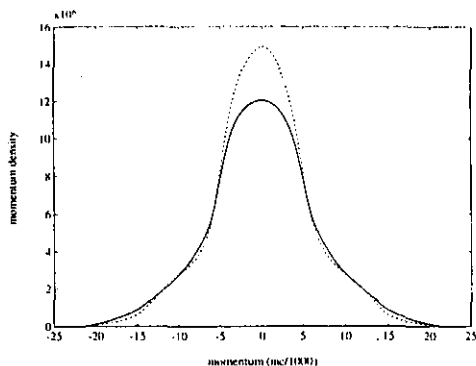
Figure 4. c-axis projection of the ACAR spectra (arbitrary units) in Γ–S direction calculated with (dashed line) and without (solid line) enhancement.
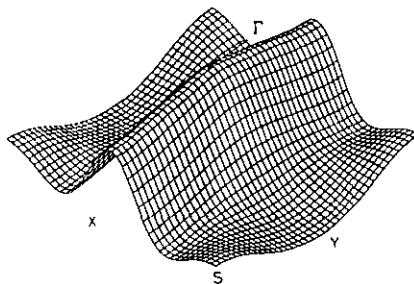
Figure 5. Calculated LCW momentum spectrum with enhancement effect and convoluted with an experimental resolution 0.5 $(mc/1000)$ $(0.001\,mc$, where m is the electron mass and c the speed of light, is equal to 1 mrad). The labels are made to be compatible with those of the simple orthorhombic Brillouin zone.

of electron and positron wavefunctions in the open spaces or on the enhancement effects.

Precise comparisons between experiment and theory are often done for the extended zone anisotropies along symmetry lines. These structures are consequences of both FS and wavefunction modulation effects. In figure 6, the Γ–Y minus Γ–X anisotropies are shown. The upper curve is from the full calculation, while in the lower one the s contributions from empty spheres and Cu p are taken out. The latter procedure was inspired by the discussion around figure 3(*b*), where it was argued that the positron at the empty site probably should swell out into the open space in the centre, if the basis had included a central s state. We therefore believe that the empty-sphere overlap with the positrons is overestimated. Hence, to estimate this effect, we reduce the s contribution and also the Cu p contribution, since it is the most extended state close to the empty sphere. From figure 6, we conclude that the wavefunction anisotropies become weak in the third zone, and the bump near 12.4 mrad is an FS effect. A similar argument has been used by Haghighi *et al* to show experimentally the existence of the ridge in the 1:2:3 compound [5].
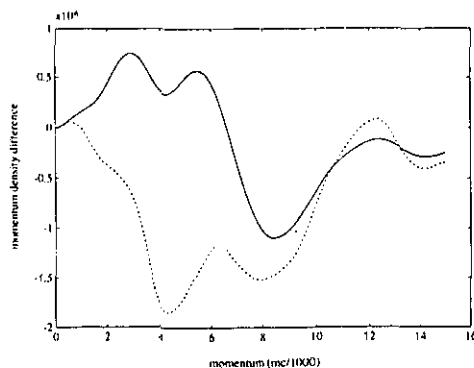

Figure 6. Γ–Y minus Γ–X anisotropies (arbitrary units): full calculation (solid line), s contributions from empty spheres and Cu p are taken out (dashed line). A small broadening function has been included in the two cases. The ridge FS break is near Γ in the first zone, near $0.0062\,mc$ in the second and near $0.0124\,mc$ in the third zone.

It seems difficult to make large single crystals of the 1:2:4 material, and experimental ACAR data are as yet unknown to us. On small polycrystals the Geneva group has been able to perform lifetime measurements, as quoted above. On the basis of these results, our calculated value and the equivalent comparison for the 1:2:3 compound, we find a similar situation in 1:2:4 and in 1:2:3. Comparisons for well behaved compounds [14] indicate that calculated lifetimes are expected to agree better with measured ones than is the case in these high-T_c oxides. This leaves the impression that real materials contain a certain amount of defects, which in ACAR measurements show up as destructive interference. But in this respect 1:2:4 is not worse than 1:2:3 and in view of its otherwise attractive features such as oxygen stability and twin-free crystals, it is our hope that large enough crystals can be made and that the ridge structure can be confirmed in ACAR measurements.

4. Conclusion

The electronic structure and the positron distribution have been calculated for YBa$_2$Cu$_4$O$_8$ and show many similarities to that of the YBa$_2$Cu$_3$O$_7$ system. The difference in FS is that there are two ridge structures instead of one, but no pillbox. Our calculated FS agrees well with full potential calculations [8–10]. The electron–positron overlap is such that only the ridge (but not the barrel) is easily detectable in ACAR measurements. The comparison between the two systems indicates that the 1:2:4 compound should give stronger ridge FS signals in LCW spectra (by a factor of two). The exact shapes of electron and positron wavefunctions in the open spaces and the enhancement effects are not crucial for the LCW spectra. But they are important for ACAR anisotropies in the low-momentum region. Experimental confirmation of our calculated predictions depends on the possibility of surmounting the difficulty of making large enough crystals.

Acknowledgments

References

[1] Jarlborg T, Barbiellini B, Boronski E, Genoud P and Peter M 1991 *J. Phys. Chem. Solids* **52** 1515
[2] Barbiellini B, Genoud P, Lerch P, Jarlborg T and Peter M 1992 *Proc. 9th Int. Conf. on Positron Annihilation (Szombathely); Material Science Forum* vol 105–110 ed Zs Kajcsos and Cs Szeles (Zurich: Trans Tech) p 599
[3] Barbiellini B, Genoud P, Henry J Y, Hoffmann L, Jarlborg T, Manuel A A, Massidda S, Peter M, Sadowski W, Scheel H J, Shukla A, Singh A K and Walker E 1991 *Phys Rev* B **43** 7810
[4] Peter M, Manuel A A, Hoffmann L and Sadowski W 1992 *Europhys. Lett.* **18** 313
Hoffmann L, Sadowski W, and Peter M 1992 *Proc. 9th Int. Conf. on Positron Annihilation (Szombathely); Material Science Forum* vol 105–110 ed Zs Kajcsos and Cs Szeles (Zurich: Trans Tech) p 411
[5] Haghighi H, Kaiser J H, Rayner S, West R N, Liu J Z, Shelton R, Howell R H, Solal F and Fluss M J 1991 *Phys. Rev. Lett.* **67** 382

[6]   Smedskjaer L C, Bansil A, Welp U, Fang Y and Bailey K G 1992 *Physica* C **192** 259
[7]   Karpinski J, Kaldis E, Jilek E, Rusiecki S and Bucher B 1988 *Nature* **336** 660
[8]   Oguchi T, Sasaki T and Terakura K 1990 *Physica* C **172** 278
[9]   Yu J, Park K T and Freeman A J 1991 *Physica* C **172** 467
[10] Ambrosch-Draxl C, Blaha P and Schwarz K 1991 *Phys. Rev.* B **44** 5141
[11] Andersen O K 1975 *Phys. Rev.* B **12** 3060;
        Jarlborg T and Arbman G 1977 *J. Phys. F: Met. Phys.* **7** 1635
[12] Jarlborg T and Singh A K 1987 *Phys. Rev.* B **36** 4660
[13] Singh D, Pickett W E, Cohen R E, Krakauer H and Berko S 1989 *Phys. Rev.* B **39** 9667
[14] Barbiellini B, Genoud P and Jarlborg T 1991 *J. Phys.: Condens. Matter* **3** 7631
[15] Kaiser J H, West R N and Shiotani N 1986 *J. Phys. F: Met. Phys.* **16** 1307
[16] Lock D G, Crisp V H and West R N 1973 *J. Phys. F: Met. Phys.* **3** 561
[17] Singh A K and Jarlborg T 1985 *J. Phys. F: Met. Phys.* **15** 727
[18] Rojas H, Barbiellini B and Jarlborg T 1992 *Proc. 9th Int. Conf. on Positron Annihilation (Szombathely);
        Material Science Forum* vol 105–110 ed Zs Kajcsos and Cs Szeles (Zurich: Trans Tech) p 799
[19] Jarlborg T 1988 *Solid State Commun.* **67** 297
[20] Barbiellini B, Jarlborg T, Gauthier M and Shukla A 1992 *Helv. Phys. Acta* **65** 840
        Gauthier M 1991 *Arch. Sci. Genève* **44** 341
[21] Nieminen R M 1991 *J. Phys. Chem. Solids* **52** 1577
[22] Hoffmann L and Manuel A A 1992 private communication